PROBLEMY MECHATRONIKI
UZBROJENIE, LOTNICTWO, INŻYNIERIA BEZPIECZEŃSTWA

ISSN 2081-5891

13, 1 (47), 2022, 45-56

PROBLEMS OF MECHATRONICS
ARMAMENT, AVIATION, SAFETY ENGINEERING

Determination of Ranges of Unstable Operation of Axial Compressor for Aircraft Turbine Engines

Adam KOZAKIEWICZ*, Maciej ADAMCZYK, Maciej MAJCHER

Military University of Technology,
Faculty of Mechatronics, Armament and Aerospace Technology
2 Sylwestra Kaliskiego Str., 00-908 Warsaw, Poland
**Corresponding author's e-mail address and ORCID*:
adam.kozakiewicz@wat.edu.pl; https://orcid.org/0000-0002-1377-5046

Received: August 15, 2021 / Revised: September 1, 2021 / Accepted: March 10, 2022 / Published: March 31, 2022

DOI 10.5604/01.3001.0015.8103

Abstract. Currently, strict requirements are set for aircraft turbine engine performance, which requires introducing larger, more complex, and more loaded compressors. In sub-assemblies designed in this manner, a vital challenge is to maintain stable compressor operation across wide range of operating conditions. This article presents the results of analysis and estimation of the range of unstable operation of an example axial compressor for a turbofan jet engine with high mass flow ratio. The analyses and numerical simulations performed made it possible to estimate the limit performance for compressor operation for two particularly important phases of flight.
Keywords: mechanical engineering, aviation, aircraft engines, stall, compressor

1. INTRODUCTION

Unstable operation of compressors is currently one of the essential phenomena in aircraft turbine engines which poses a risk for flight safety and causes numerous problems in aircraft operation [1]. Unstable compressor operation results mainly from disturbances in air flow through the engine duct. During normal operation, such disturbances may occur upon a change in angle or velocity of the airflow supplied to the inlet while manoeuvring, or during engine acceleration and deceleration. Increasing instability of compressor operation may cause a serious threat to flight operation safety due to the loss of thrust, damaged sub-assemblies or complete engine shutdown. If a compressor operates in an unstable manner, it loses its capacity to force air flow along the engine duct. Intensification of this phenomenon leads to the engine surge – in this state, high pressure air accumulated in the middle section is ejected simultaneously through the inlet and outlet (Figure 1).

Fig. 1. Unstable compressor operation in a Boeing 777 leading to flame outburst [2]

The issue of compressors stall in turbine engines appeared in aviation as early as when the compressors were put into operation. The primary cause of this phenomenon in axial compressors is the separation airflow on rotor blades. Separations may originate from disturbances in the airflow supplied through the intake system and may be caused e.g. by blasts of wind, turbulence, or changes in the engine rotational speed. They may also occur after manoeuvres, e.g. on changing angle of attack or angle of slip. In turbofan jet engines, due to the large diameters of the intake systems, the main situations in which compressor stall may occur include landing at cross-wind and manoeuvring at large angles of attack.

Due to the significant curvature of the engine nacelles, separations and areas of disturbances occur at the internal side of the inlet when the airflow to the inlet is not uniform. In extreme cases, significant acceleration of the stream in this area may cause the speed of sound to be exceeded locally and the formation of a lambda shockwave, which may lead not only to propagation of the disturbance down into the duct, but also to damage to its components, specifically fan blades [4]. An example of the above disturbances is provided in Figure 2.

The aim of this article is to present the results of the analysis and to estimate the range of unstable operation of the axial compressor. The analysis was performed on an example of a turbofan jet engine with three rotors and with a high mass flow ratio. These units are commonly used in commercial aviation as power plants for wide-body long-haul aircraft. The geometry of the tested model and the selected air flow parameters may be compared to the results presented in the publication covering the Trent 1000 [5] – an engine popular in commercial aviation. Similar analyses for compressors with different parameters and designs are discussed e.g. in publications [6, 7].

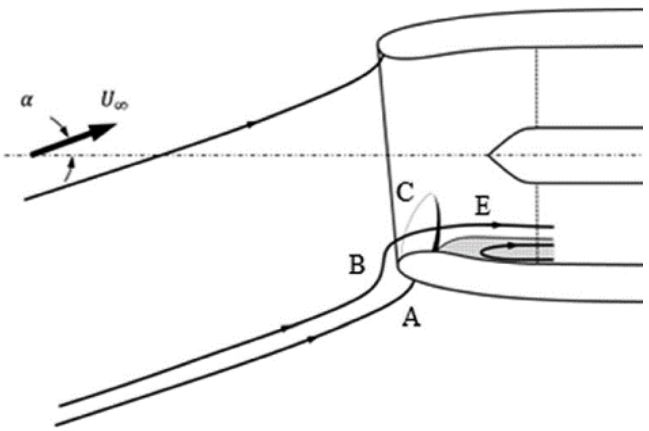

Fig. 2. Diagram of operation of an inlet of an engine with a high angle of attack, α – angle of attack, A – pressure increase point, B – flow round the bottom nacelle curvature, C – λ shock wave, E – flow separation area [3]

2. DETERMINATION OF COMPRESSOR PERFORMANCE

First, calculations to determine the duct and compressor blade geometry were performed. Geometry of the compressor, including rotors and stators, was specified based on the methods described in references [8, 9] and using the structural assumptions provided in Table 1.

Table 1. Input parameters for compressor calculations

Rotor rotational speed [rpm]	n	8937.0
First stage reaction [-]	ρ	0.54
Compression ratio [-]	π_S^*	8.89
Mass flow rate [kg/s]	$\dot{m}$	110.0

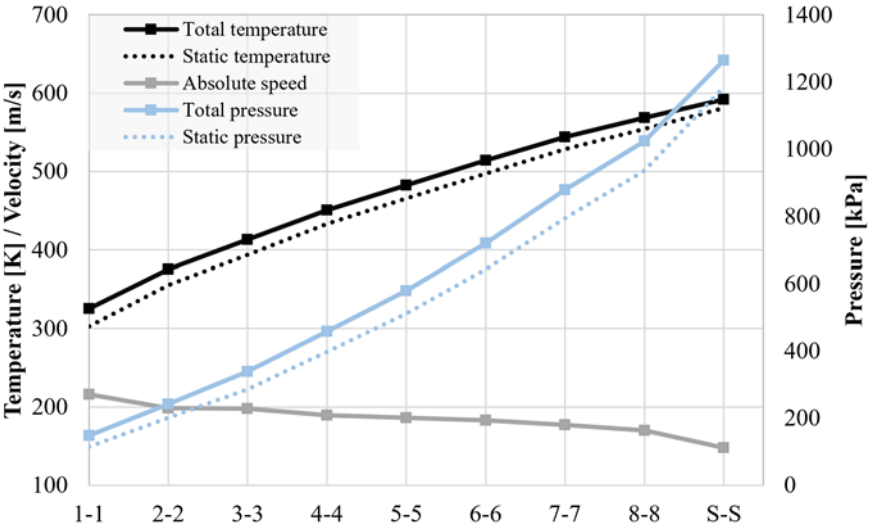

Fig. 3. Stream parameters for individual compressor stages

Based on the assumptions accepted (Table 1), a concept of an eight-stage intermediate pressure compressor (IPC) with three transsonic stages was developed. The compression ratio at the first stage under design conditions was 1.65, which is a typical value for transsonic stages. Main parameters of the stream along the duct are presented in Figure 3. The results obtained were used to determine the compressor characteristics using GasTurb 13. Figure 4 presents normal characteristics for compressor operation under static conditions, with an operating line of the compressor with the turbine. This relationship is reflected in equation (1).

$$\frac{\pi_S^*}{q(\lambda_1)} \approx b\sqrt{\frac{e_S^* - 1}{\eta_S^*}} \tag{1}$$

where: π_S^* – compressor ratio, η_S^* – compressor efficiency, $e_S^* = \pi_S^{*\frac{k-1}{k}}$, b – constant being the function of engine duct cross-sectional area, pressure loss and efficiency coefficients, and constant coefficients for air and flue gas, $q(\lambda)$ – compressor reduced speed function.

The presented characteristics indicate that the compressor has insufficient stall margin in the low speed range, n = 52.8%÷66.1%, i.e. where the operating line is close to or exceeds the surge line. This is an important area for scientific research from the perspective of stability of operation of the compressor and the entire engine. Such issues are the subjects of interest in numerous scientific centres, such as Massachusetts Institute of Technology, Cambridge University, and NASA, which cooperate in this respect with aviation industry leaders, i.e. Pratt & Whitney, General Electric, Collins Aerospace, Rolls-Royce, and Safran Group.

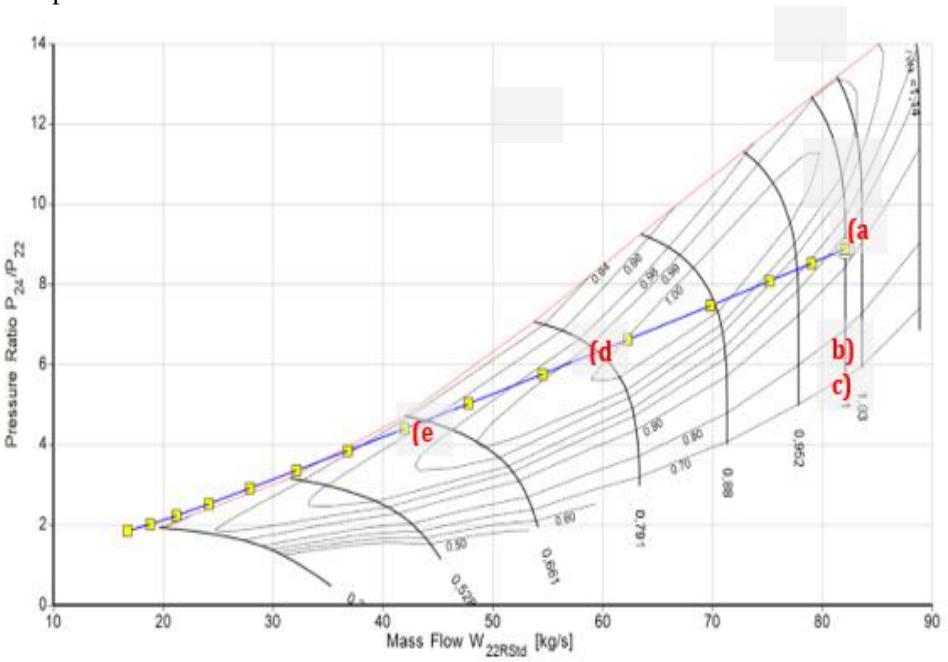

Fig. 4. Compressor map with operating line

3. MODEL DESIGN

Further analysis was related to the design of a numerical model of the compressor's stage using Ansys. A two-dimensional model of the compressor's stage was designed based on the assumptions stemming from the model of a straight-line palisade. It was prepared in such a manner that the so-called periodic boundary conditions are applied. The periodic boundary conditions are used in design cases when the expected model of a flow solution is repeatable and period, as in the case of the compressor being an example of an axial fluid flow machine. The application of periodic boundary conditions allows the time to be shortened for both mesh generation and the numerical simulations without any loss of physical properties of the flow phenomena.

Therefore, it was possible to model individual design areas for an inlet guide vanes comprising a single airfoil, a rotor and stator represented by two airfoils. NACA 16-006 airfoil was adopted for the numerical simulations. Airfoil chords and angles resulted from the analytical dry gas calculations for the medium cross-section. As a result, the inlet guide vane airfoil angle was 46.41 degrees, the rotor angle was 43.04 degrees, whereas the stator angle was 45.92 degrees. The width of the palisade resulting from the calculated palisade pitch was: for the inlet guide vanes – 109.78 mm, for the rotor – 77.49 mm, and for the stator – 89.87 mm.

Table 2. Mesh parameters

Max. skewness	0.64247
Min. orthogonality	0.57933
Number of nodes	16,989
Number of elements	32,530

The prepared model of a straight-line palisade in the form of a set of planes was subject to discretisation in Ansys Workbench (Mesh module). For the purposes of the computational model discretisation, the so-called hybrid mesh was used – this mesh is a peculiar compromise between structural and non-structural meshes. In the area of the wall layer, five layers of prismatic elements were modelled, whereas the remaining computational area was discretised using triangular elements. Main parameters and indicators of the mesh quality are provided in Table 2, whereas the computational model of the stage and its discretisation are presented in Fig. 5.

At first, simulation was performed for the design conditions of an engine operating on the ground (as a reference). Then the mass flow rate was decreased (specified in the model as a vector c_{1a}) or the rotor's rotational speed (designated with vector U) to determine the effect of these changes on the condition of the palisade. Both vectors are crucial to establish the conditions of the compressor's operating point (Figure 4), which translates into the conditions of stream flow around the compressor blades [10]. The relationship between speed components and compression can be described using equation (2).

$$\frac{c_{an}}{c_{aI}}\pi_S^{\frac{1}{n}} = idem \tag{2}$$

where: c_{an} – axial speed at outlet, c_{al} – axial speed at inlet, n – real transformation exponent, π_S – compressor compression.

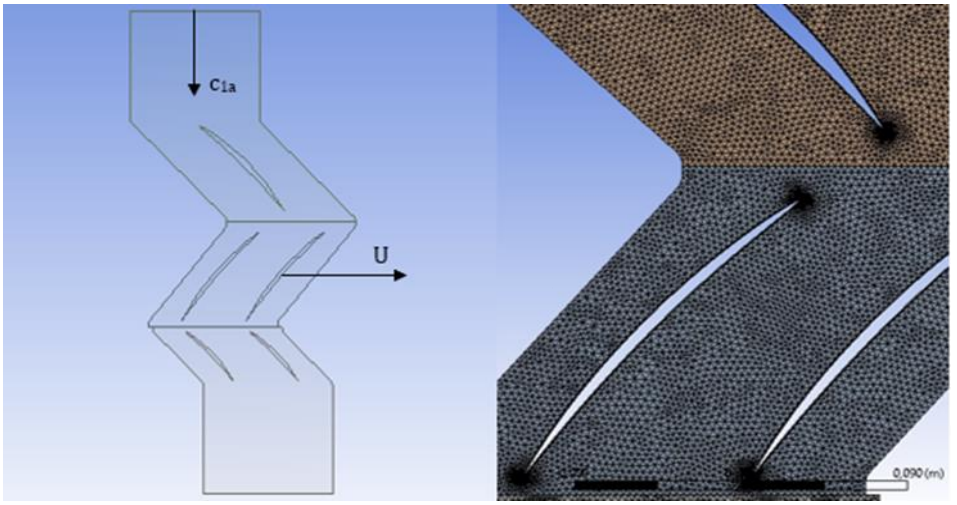

Fig. 5. Computational model of the stage and generated mesh

The change in axial speed vector c_{1a}, which in this case reflects the change in mass flow rate in the compressor, may occur while manoeuvring an aircraft, as a result of modification of the engine nacelle's angle of attack, e.g. while climbing or descending at a constant engine speed. The second important control parameter of the turbine engine is the rotational speed (Figure 4). A change in this parameter is reflected by a change in peripheral speed vector of the rotor in the model developed (Figure 5). For the numerical tests, two design cases were selected based on a literature analysis:

1) Mass flow rate decrease at constant rotor speed ($c_{1_a} < c_{1_{a_O}}$, $U=U_o$)
2) Rotor speed decrease at constant mass flow rate ($c_{1_a} = c_{1_{a_O}}$, $U<U_o$)

4. RESULTS

Numerical simulations were performed using the k-ω SST model. Values of boundary conditions for the model are provided in Table 3.

Table 3. Boundary conditions for computational domain

Inlet static pressure	p_1	139.0 [kPa]
Outlet static pressure	p_2	200.8 [kPa]
Stream axial speed	c_{1_a}	184.3 [m/s]
Peripheral speed [m/s]	U	392.5 [m/s]

The results of numerical simulations in the form of raster diagrams for the first case are presented in Figure 6. The results of static pressure are presented with reference to the static conditions on the ground. Variable conditions of engine operation were modelled with a change in the mass flow rate. It was reflected by axial speed vector c_{1a} which was decreased subsequently by 20% and 40% with reference to the engine design conditions (c_{1_a}=184.3 m/s) while keeping the rotor speed constant (U = 392.5 m/s).

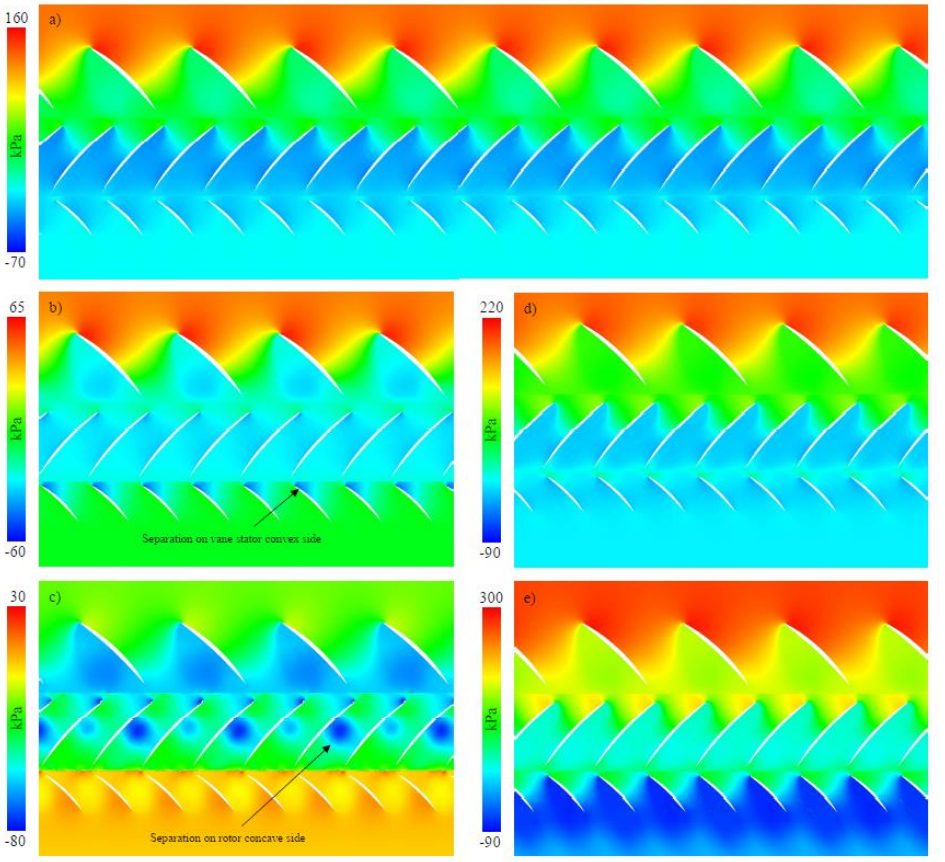

Fig. 6. Static pressure of the palisade at a decreased mass flow rate and rotor speed: a) – design conditions, b) – mass flow rate decreased by 20%, c) – mass flow rate decreased by 40%, d) – rotor speed decreased by 20%, e) – rotor speed decreased by 40%

At the computational point, the palisade is stable (Figure 6.a). According to the numerical simulations, for such engine conditions, compression ratio of the stage was $\pi_I^* = 1.65$, which matches the result of the analytical conditions. At a decreased mass flow rate by 20%, the palisade remains stable, but a pressure drop at the outlet is observed (Figure 6.b).

For this case, the value of compression ratio was $\pi_I^* = 1.24$. Moreover, due to overall changes in flow kinematics through the palisade, a separation at the stators' leading edge can be noticed. At a decreased mass flow rate by 40%, loss of the palisade's stability can be observed (Figure 6.c). It loses the capacity to force air to flow along the engine duct. A considerable vacuum area is formed on the concave side of the rotor blades. Flow is disturbed and compression ratio of the stage is reduced to $\pi_I^* = 0.92$. This case is associated with points designated as b) and c) on the compressor characteristics (Figure 4), respectively. They indicate moving close to the compressor's lower choke line.

The results of numerical simulations for the second case are presented in Figure 6. Rotor speed, shown in the model using speed vector *U*, decreased subsequently by 20% and 40% with reference to the engine design conditions while keeping the inlet stream speed constant (c_{1_a}=184.3 m/s, U = 392.5 m/s).

At the computational point, the palisade is stable (Figure 6.a). At a decreased rotor speed by 20%, the first signs of unstable operation of the compressor stage in the form of separations on the stator blade concave side appears and stage compression ratio drop occurs. At a decreased rotor speed by 40% with reference to the design conditions, the stage's capacity to force air to flow along the engine duct is completely lost. The value of compression ratio drops below unity, and great areas of separation occur at the rotor and the stator, leading to a complete flow blockage and choke. The results in this respect comply with the determined compressor characteristics. This corresponds to points d) and e) on the characteristics (Figure 4), respectively. They indicate moving close to the surge line within the range of low rotational speeds.

Figure 7 presents the relative speed of stream at the rotor for cases involving mass flow rate decrease and rotor speed decrease.

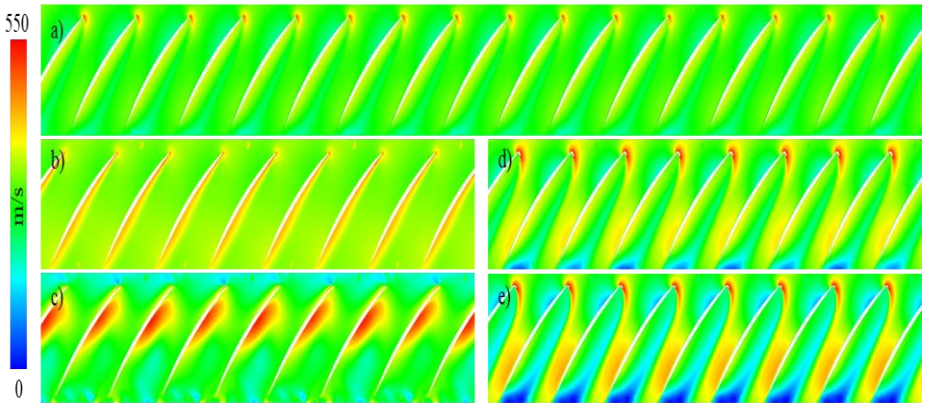

Fig. 7. Relative speed of the rotor at a decreased mass flow rate and rotational speed: a) – design conditions, b) – mass flow rate decreased by 20%, c) – mass flow rate decreased by 40%, d) – rotor speed decreased by 20%, e) – rotor speed decreased by 40%.

In the case of a mass flow rate decrease (Figures 7.b, 7.c), significant speed increases can be observed in areas of separation – they are greater when the mass flow rate through the palisade decreases. In the case of rotor speed decrease (Figures 7.d, 7.e), strong separation originating at the blade leading edge and propagating along the passage on its internal (concave) side can be noticed. This results in a complete blockage of the passage.

5. CONCLUSIONS

The results obtained show that as far as the stage of the turbofan jet engine is concerned, unstable operation begins at lowering the mass flow rate by 40% while maintaining a constant rotor rotational speed. Such a situation may occur while climbing at large angles of attack and corresponds to points b) and c) indicated in the compressor characteristics (Figure 4).

Unstable compressor operation in this case is a dangerous phenomenon since separations begin to form on the rotor blade convex side, which may lead to immediate propagation of the disturbance inside the compressor duct on the remaining stages. Unstable operation in the second case can be noticed when rotor speed is decreased by 40% while keeping the inlet air speed constant. Such a situation occurs while descending and corresponds to points d) and e) indicated in the compressor characteristics (Figure 4).

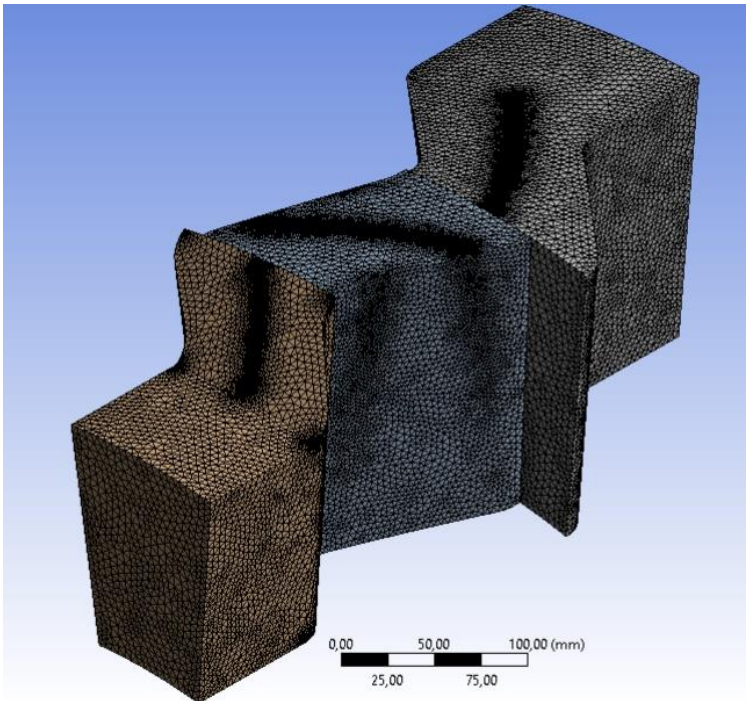

Fig. 8. Extension of the palisade model to a three-dimensional model

Here, the resulting disturbance is less dangerous since separations are formed on the rotor concave side, which means they are compensated by rotational movement of the blades in this direction.

It should be noted that the compressor characteristics does not include the operation of systems ensuring stability and preventing unstable operation, which in modern designs are very advanced (i.e. variable guide vanes and air bleeds), and the numerical model is significantly simplified. In the following stage, the authors will develop this issue in a three-dimensional model (Figure 8). Numerical simulations for this three-dimensional model will allow for a more accurate analysis of flow phenomena occurring at the compressor stage.

FUNDING

The authors received no financial support for the research, authorship, and/or publication of this article.

REFERENCES

[1] Balicki, Włodzimierz, Ryszard Chachurski, Krzysztof Kawalec, Adam Kozakiewicz, Stefan Szczeciński. 2010. „Praca niestateczna silników turbinowych – przyczyny powstawania i sposoby zapobiegania". *Prace Instytutu Lotnictwa* 199 : 50-55.

[2] El-Sayed, F. Ahmed. 2016. *Fundamentals of Aircraft and Rocket Propulsion*. Londyn: Springer.

[3] Kalsi, S. Hardeep, Paul G. Tucker. 2018. Numerical Modelling of Shock Wave Boundary Layer Interactions in Aero-engine Intakes at Incidence. In *Proceedings of ASME Turbo Expo 2018 Turbomachinery Technical Conference and Exposition*, June 11–15, 2018 Oslo, Norway.

[4] Carnevale, Mauro, Feng Wang, Luca di Mare. 2017. "Low Frequency Distortion in Civil Aero-engine Intake". *Journal of Engineering for Gas Turbines and Power* 139 (4) : 041203-1-12.

[5] El-Sayed, F. Ahmed, Mohamed S. Emeara, Islam Mohamed Asoliman, Mohamed Ehab, Abdullah M. Mahrous. 2018. Performance Analysis of High Bypass Turbofan Engine Trent 1000-A. In *Proceedings of the IUGRC International Undergraduate Research Conference*. Egypt, Cairo, July, 2018.

[6] Kumar, Lakshya, Dilipkumar B. Alone. 2019. Design and CFD Analysis of a Multi Stage Axial Flow Compressor. In *Proceedings of the 21st Annual CFD Symposium*. CFD Division Aeronautical Society of India 08 – 09 August, 2019 Bangalore.

[7] Cornelius, Christian, Thomas Biesinger, Paul Galpin, Andre Braune. 2014. "Experimental and Computational Analysis of a Multistage Axial Compressor Including Stall Prediction by Steady and Transient CFD Methods". *Journal of Turbomachinery* 136 (6) : 061013-1-12.
[8] Dzierżanowski, P., J. Otyś, S. Szczeciński, R. Wiatrek. 1972. *Konstrukcja silników lotniczych. Projektowanie przejściowe i dyplomowe*. Warszawa: Wydawnictwo Wojskowej Akademii Technicznej.
[9] Antas, Stanisław, Piotr Wolański. 1989. *Obliczenia termogazodynamiczne lotniczych silników turbinowych*. Warszawa: Politechnika Warszawska.
[10] R. Wiatrek. 1983. *Teoria Silników Lotniczych*. Warszawa: Wydawnictwo Wojskowej Akademii Technicznej.
[11] Kurzke, Joachim, Ian Halliwell. 2018. *Propulsion and Power. An Exploration of Gas Turbine Performance Modeling*. Londyn: Springer.
[12] *Ansys Fluent 12.0, User's Guide*. 2009.

Wyznaczanie zakresów niestatecznej pracy sprężarki osiowej lotniczych silników turbinowych

Adam KOZAKIEWICZ, Maciej ADAMCZYK,
Maciej MAJCHER

Wojskowa Akademia Techniczna
ul. gen. Sylwestra Kaliskiego 2, 00-908 Warszawa

Streszczenie. Współcześnie stawia się wysokie wymagania wobec parametrów osiąganych przez lotnicze silniku turbinowe, co powoduje konieczność wprowadzania do konstrukcji coraz większych, bardziej skomplikowanych i obciążonych sprężarek. W tak projektowanych podzespołach istotnym wyzwaniem jest zachowanie stabilności pracy sprężarki w szerokim zakresie warunków operacyjnych. W niniejszym artykule przedstawiono wyniki analizy i oszacowania zakresu niestatecznej pracy przykładowej sprężarki osiowej do dwuprzepływowego silnika turbinowego o dużym stopniu podziału masowego natężenia przepływu. Przeprowadzone analizy i obliczenia pozwoliły na oszacowanie granicznych parametrów pracy sprężarki dla dwóch szczególnie istotnych faz lotu samolotu.
Słowa kluczowe: inżynieria mechaniczna, lotnictwo, silniki lotnicze, pompaż, sprężarki